

Progress report on XMaS U/Fe multilayer measurements and analysis

S. D. Brown, L. Bouchenoire, A. Mirone and V. Cotroneo

Background

Initial attempts to fit the reflectivity data of Fig 1 from sample 2.9, a nominal $[U_{30} \text{ \AA} / Fe_{40} \text{ \AA}] \times 30$ multilayer, failed to reproduce the dip at the first superlattice peak position. A good knowledge of the chemical structure is required, together with accurate values for f' and f'' , in order to model the distribution of uranium magnetic moments within the multilayer.

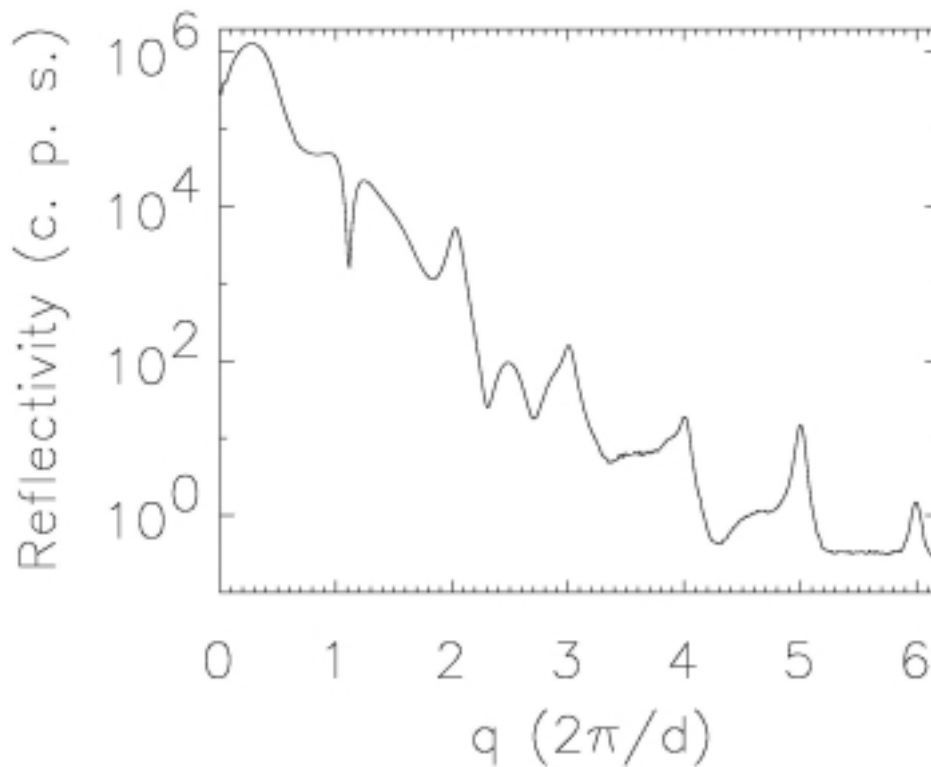


Fig 1. Reflectivity at the uranium M_{IV} edge. The problem has been modelling the dip at the first superlattice peak position.

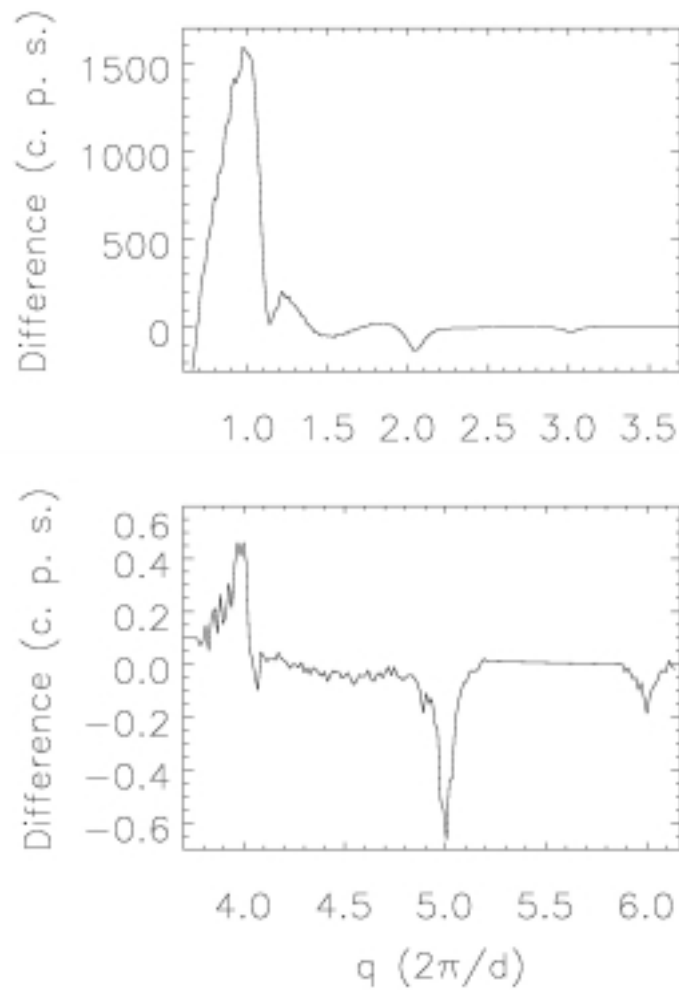


Fig 2. Measured magnetic difference signal for the first to sixth superlattice reflections.

The measured magnetic difference signal follows the sequence + - - + - - from the first to sixth superlattice reflections respectively, as shown in Fig 2. Without a detailed knowledge of the chemical structure it is not possible to fit this data reliably and all that can be deduced is that the uranium moments must be highly non-uniformly distributed within the multilayer.

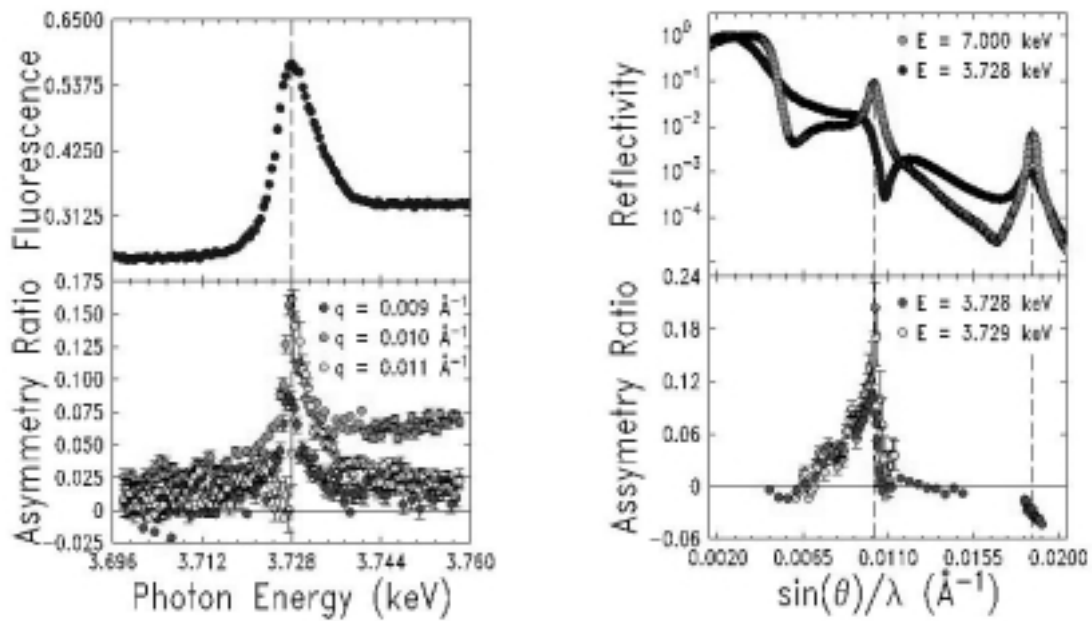


Fig 3. The energy (left) and q (right) dependence of the magnetic asymmetry ratio.

The magnetic asymmetry ratio was found to vary rapidly with both photon energy and q , as illustrated in Figs 3 and 4. In order to obtain a reliable representation of the sample reflectivity and magnetic signal, an energy versus q grid of data were captured with a high point density around the edge and lower point density away from the edge. Any other approach could lead to aliasing of any q or energy dependent fit.

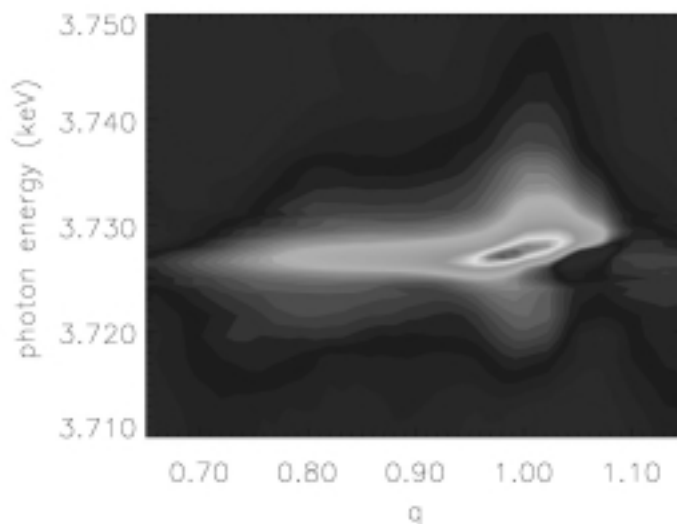


Fig 4. Asymmetry ratio around the first magnetic reflection.

Method

The measured sample fluorescence was rescaled and tied to tabulated absorption values away from the uranium M_{IV} edge in order to give a measure of f'' . The ‘white-line’ in the absorption then corresponded to about 50 electrons. Kramers-Kronig transformation led to a knowledge of f' . However, as previously stated, no reasonable fit to the data for Fig 1

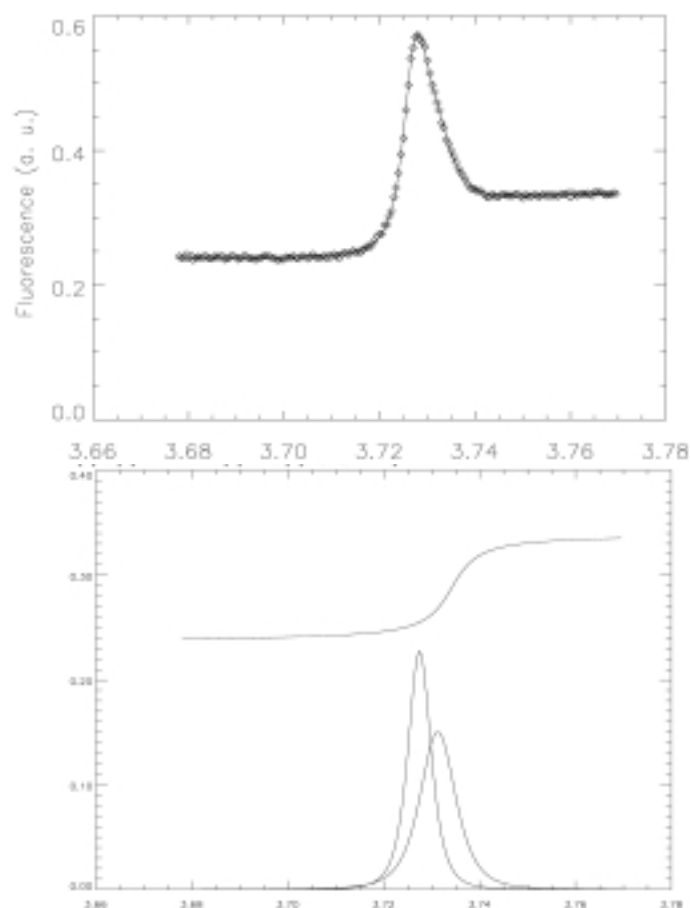


Fig 5. Upper panel: The measured sample fluorescence (points) and the parameterised fit (line). Lower panel: The fit broken down into its constituent parts.

could be obtained. We know that *some* of the uranium in the multilayer is ferromagnetic but the fluorescence data comes from *all* of the uranium within the multilayer and therefore may be unreliable as a measure of f'' at the interfaces, where the reflectivity takes place. In order to allow variation of f'' (and f' through Kramers-Kronig transformation) in the fitting program, it was decided that the fluorescence data should be parameterised. Fig 5 shows the sum of an arctan function and a Lorentzian squared line centred on the absorption edge and a second Lorentzian squared line shifted to higher energy. This seemed to provide an accurate fit to the measured sample fluorescence.

Results

Reflectivity data captured at 10keV and 7 keV were simultaneously fitted with a model consisting of a multilayer stack with the top two bilayers expanded and also a perturbed bilayer at the substrate interface. The data were captured at different times and possibly at different points on the sample which could explain why we were unable to fit the two data sets with a one model. However, the model described above was found to fit both data sets if small changes in the thicknesses and densities of the top bilayers were allowed (this may also be due to some time dependant sample degradation). This model was then simultaneously applied to 27 reflectivity curves taken around the uranium M_{IV} edge and fitted, along with the parameterised f'' (and resultant f') model (the 10 keV data were also simultaneously fitted, this data set being more recent than the 7 keV data). The resultant fit, together with the uranium M_{IV} edge experimental data are shown in Figs 6 to 8.

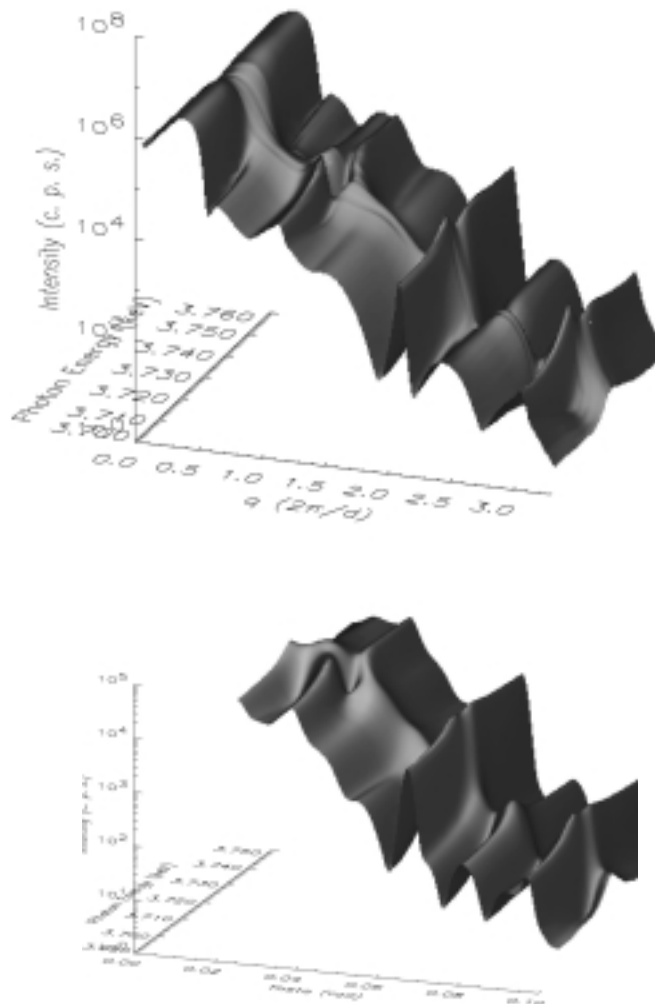


Fig 6. Experimental data (upper plot) and the fitted model data (lower plot) described in the text. The lower angle data was not included in the fit due to sample footprint effects.

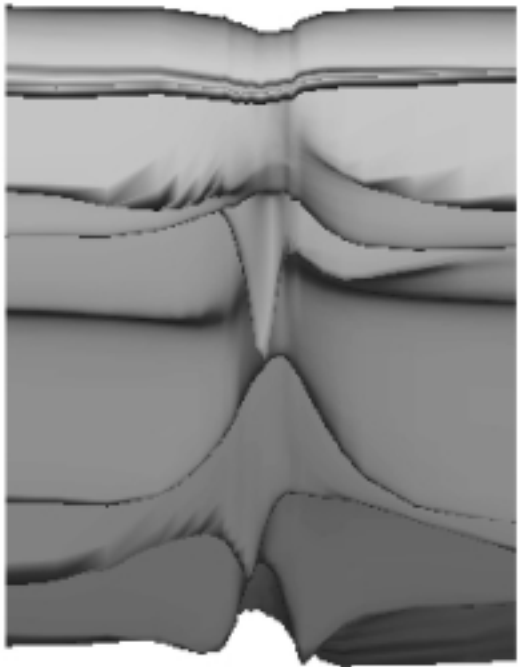


Fig 7. As Fig 6 but viewed from behind, looking along the q direction. The experimental data is to the right and the result of the fit is on the left. The fit is underestimating the sharpness of the dip but agreement is reasonable.

Seven ESRF computers running a total of 14 different processors in parallel were employed to reduce the considerable times required for parameter optimisation. Although not perfect, the agreement between the experimental data and the fit results is reasonable and can now easily be improved through further refinement of the multilayer model.

31st March 2004

Fig 8. Experimental data (upper plot) and the fitted model data (lower plot). This view clearly shows the anomalous shift between the pre and post-edge peak positions, indicating good agreement between actual and modelled f' and f'' .

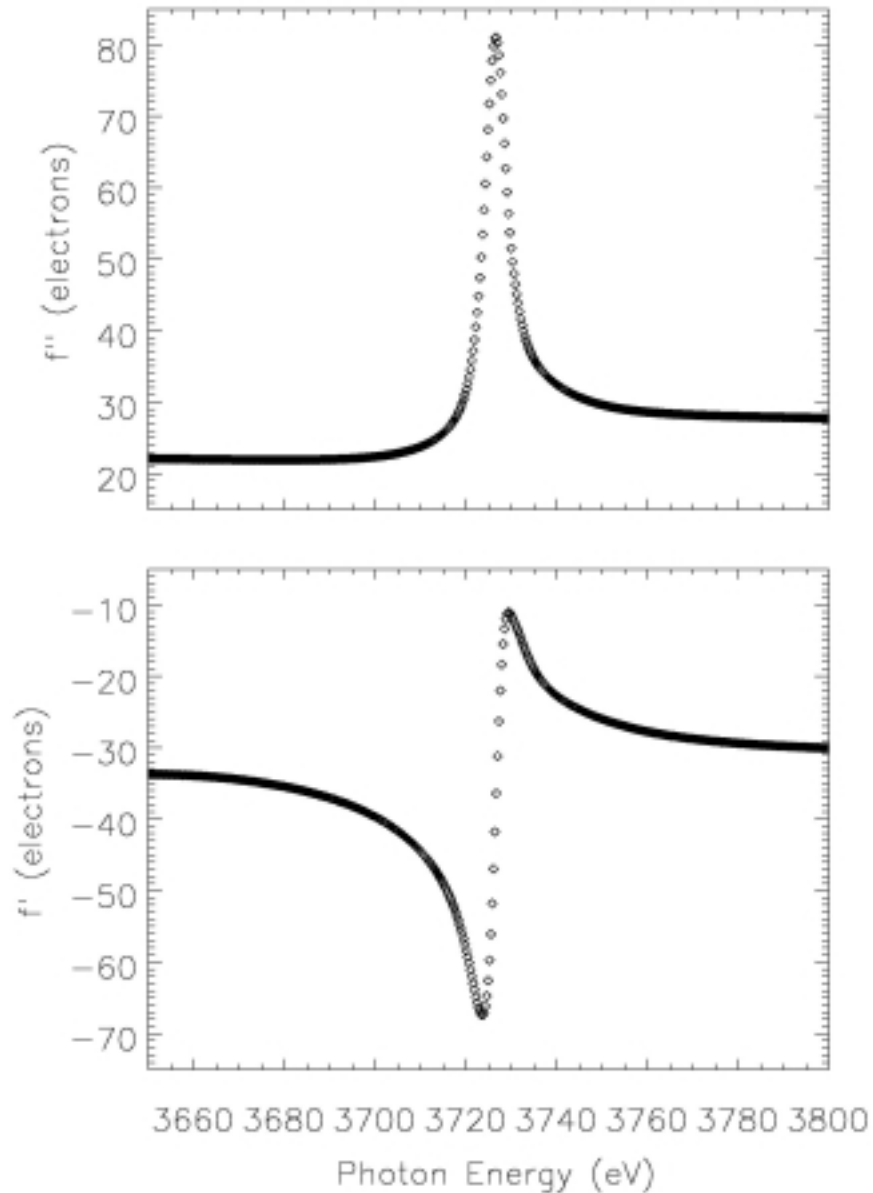


Fig 9. Real (lower plot) and imaginary (upper plot) parts of the uranium M_{IV} anomalous scattering factor extracted through parameterisation of fluorescence data and subsequent fitting to reflectivity data.

The fitted f' and f'' curves are shown in Fig 9. The program has independently increased the number of electrons from 50 to around 80, which is in general agreement with the published values for f'' in UO_2 . The consequent values for f' are also consistent with those reported for UO_2 .

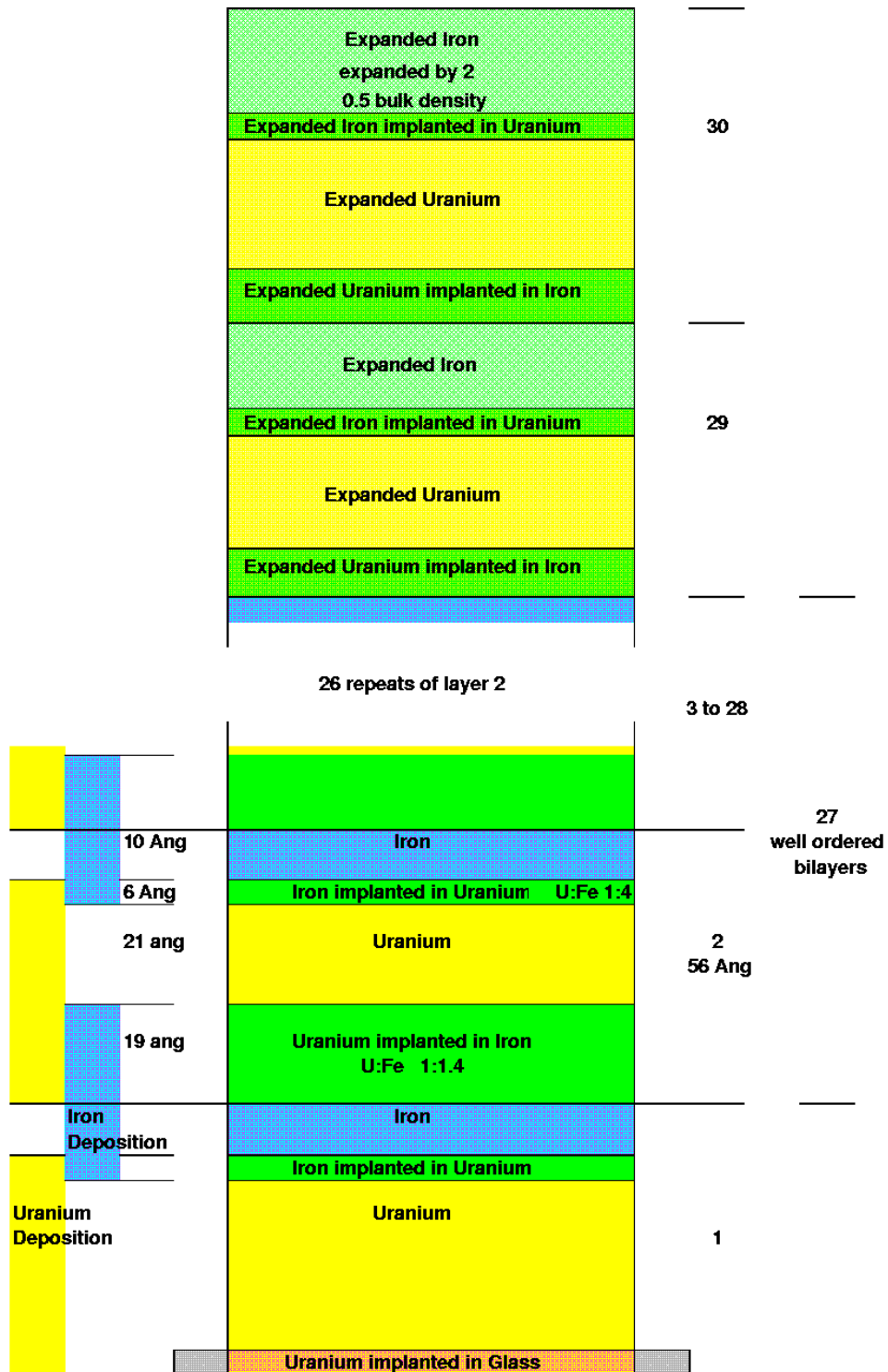


Fig 10. The fitted model, including two expanded (oxidised) bilayers at the top and the perturbed bilayer at the glass interface.

The resultant model multilayer structure is shown in Fig 10, with a representation of the deposited layer thickness depicted to the left of the figure. The deposition progresses as follows:

Firstly, 38 Å of uranium is sputtered onto the glass substrate. The 7 and 10 keV reflectivity data sets required a uranium implanted glass layer of thickness 5 Å at the uranium/glass interface in order to provide an adequate fit (the M_{IV} reflectivity is oblivious to this interface, due to high sample absorption). Secondly, 35 Å of iron is sputtered onto the uranium layer, which implants itself into the uranium to a depth of around 6 Å. Next, 46 Å of uranium is sputtered onto the remaining 29 Å of pure iron, which implants itself into the iron to a depth of 19 Å, resulting in a 27 Å pure uranium layer. Finally, the another 35 Å of iron is sputtered onto the uranium, again implanting itself to a depth of 6 Å and with the subsequent deposition of the next uranium layer, a stable repetitive structure commences. With continuation of this deposition and implantation processes, a total of 29 periodic quadrayers are produced. However, subsequent oxidation and expansion of the top two quadrayers leaves only 27 well ordered periodic quadrayers intact.

Discussion

There are some salient features of this model, which will now be elaborated upon. Firstly, the initial uranium layer of thickness 38 Å is reduced in thickness from the 46 Å uranium deposition observed in the majority of the stack. This indicates that the initialisation of stable growth of uranium on glass, (ie the 'sticking') takes longer than it does on iron. Thus the nominal uranium thickness of 30 Å, provided through a thickness calibration of a single uranium layer on a glass substrate, is in general agreement with the model, when one subtracts the 5 Å lying within the glass ($38 - 5 = 33$ Å). However, it can be seen that the subsequent uranium layer thicknesses differs from the thickness calibration due to the different sticking coefficients for uranium on glass and uranium on iron. The uranium sticks better to the iron due to the implantation process. The depth of implantation of the uranium into iron and into glass also reflects the relative hardness of these two materials. The thickness of the iron deposition in the model is 35 Å which is also in general agreement with the nominal iron thickness of 40 Å.

Another potentially physical effect observed in the model is that uranium implants into iron to a greater depth than iron implants itself into uranium. This is consistent with the relatively large mass of the uranium atoms with respect to the iron atoms. Also, although it is difficult to differentiate between implantation and interdiffusion processes, the later would be more difficult to reconcile with the fitted periodic uranium and iron thicknesses, as the resultant period would be likely to be closer to 70 Å than the observed 56 Å.

Turning to the mixed element implanted regions, the magnetic properties of UFe in the ratios 1:1.4 or 1:4 are not known and it would be of practicable importance to study such alloys. In addition, as both the uranium and the iron are clearly unthermalised for the

31st March 2004

described implantation processes to occur, these mixed layers are likely to also be under low pressure due to thermal contraction of the stack after deposition, further complication any comparisons to UFe_2 and evaluation of T_C .

Finally, the expanded iron at the top of the stack was fitted to twice the thickness and half the density of the unexpanded iron in the periodic part of the multilayer, which is another independently fitted self-consistent result.

Future work

The fitting of the chemical structural model will continue to be refined for the next week or so, after which we will commence the magnetic structural fitting.